

# Critical temperatures of the two-band model for diluted magnetic semiconductors

F. Popescu,<sup>1</sup> Y. Yildirim,<sup>1</sup> G. Alvarez,<sup>2</sup> A. Moreo,<sup>3,4</sup> and E. Dagotto<sup>3,4</sup>

<sup>1</sup>Physics Department, Florida State University, Tallahassee, Florida 32306, USA

<sup>2</sup>Computer Science and Mathematics Division, Oak Ridge National Laboratory, Oak Ridge, Tennessee 37831-6032, USA

<sup>3</sup>Department of Physics, The University of Tennessee, Knoxville, Tennessee 37996, USA

<sup>4</sup>Condensed Matter Sciences Division, Oak Ridge National Laboratory, Oak Ridge, Tennessee 37831-6032, USA

(Received 11 October 2005; published 15 February 2006)

Using dynamical mean field theory and Monte Carlo simulations, we study the ferromagnetic transition temperature ( $T_c$ ) of a two-band model for diluted magnetic semiconductors (DMS), varying coupling constants, hopping parameters, and carrier densities. We found that  $T_c$  is optimized at all fillings  $p$  when both impurity bands fully overlap in the same energy range, namely when the exchange couplings  $J$  and bandwidths are identical. The optimal  $T_c$  is found to be about twice larger than the maximum value obtained in the one-band model, showing the importance of multiband descriptions of DMS at intermediate  $J$ 's.

DOI: 10.1103/PhysRevB.73.075206

PACS number(s): 71.27.+a, 75.50.Pp, 75.40.Mg

## I. INTRODUCTION

Diluted magnetic semiconductors (DMS) are semiconductors where a fraction  $x$  ( $\sim 0.01$ – $0.1$ ) of nonmagnetic elements is replaced by magnetic Mn ions. The class of III-V DMS has recently attracted considerable attention after the experimental observation of high  $T_c$ 's, due to significant improvements in molecular beam epitaxy techniques.<sup>1</sup> These compounds can play an important role in spintronic devices, and they represent a challenge to theory due to the combined presence of correlations and disorder.

Using a one-band model for DMS, (i) the weak-coupling quadratic dependence of  $T_c$  with  $J$  is captured correctly by dynamical mean field theory (DMFT),<sup>2</sup> which also provides bulk limit results, while (ii) the Monte Carlo (MC) techniques on finite clusters properly handle the random Mn distribution and unveiled the reduction of  $T_c$  at large  $J$  due to carrier localization.<sup>3</sup> For  $J$  comparable to the hopping  $t$ , both techniques reached similar conclusions, showing that they can complement towards a comprehensive understanding of DMS. However, much theoretical work remains to be done, particularly the consideration of the several bands active in real DMS materials beyond mean field approximations.<sup>4</sup> In this paper, we study a two-band model for DMS at realistic low dopings  $x \ll 1$ , using a combination of *nonperturbative* techniques that gives unique characteristics to our work. To properly analyze the intermediate and strong coupling  $J$  regime, MC simulations that correctly handle the random Mn distribution are crucial. Here, MC results for DMS models including more than one band are presented for the first time.<sup>5</sup> On the DMFT side, pioneering calculations for two-band double-exchange Hamiltonians already exist.<sup>6</sup> However, those calculations focused on special cases, while our current DMFT effort is more general, with two  $s=1/2$  bands and arbitrary couplings, hoppings, and carrier densities. One of our main results is that  $T_c$  can be substantially raised by considering multiband systems since at intermediate couplings the maximal  $T_c$  at carrier filling  $p \cong x$  is approximately twice larger than the highest  $T_c$  obtained in the single-band model at filling  $p \cong x/2$  (note that the alternative notation

$p_h = p/x$ , where  $p_h$  is the hole density as a fraction of  $x$ , will be used in some portions of the paper). The qualitative reason is that the impurity bands (IB) cooperate to raise  $T_c$  for values of the chemical potential  $\mu$  where those bands partially or fully overlap.<sup>7</sup>

The paper is organized as follows: Section II describes the model; the DMFT results are presented in Sec. III, while Sec. IV is devoted to the Monte Carlo study. Conclusions and final remarks are in Sec. V.

## II. MODEL

It is known that in Mn-doped GaAs, the Mn ions substitute for Ga cations and contribute itinerant holes to the valence band. The Mn ions have a half-filled  $d$ -shell which acts as a  $S=5/2$  local moment. Due to a strong spin-orbit (SO) interaction, the angular momentum  $\mathbf{L}$  of the  $p$ -like valence bands mixes with the hole spin degree of freedom  $\mathbf{s}$  and produces low- and high-energy bands with angular momentum  $j=1/2$  and  $3/2$ , respectively. A robust SO split between these bands causes the holes to populate the  $j=3/2$  state, which itself is split by the crystal field into a  $m_j = \pm 3/2$  band with heavy holes and a  $m_j = \pm 1/2$  band with light holes. This is the reason why we choose to study two bands since this is the relevant number of orbitals in most III-V DMS. Since we do not work in a  $(j, m_j)$  basis our Hamiltonian does not capture the orbital mixing in the Hund term.<sup>8</sup> However, we roughly consider the diagonal SO effects in the magnetic interactions by allowing different values of  $J$  in the two orbitals considered. The simple two-band model for DMS used here is given by the Hamiltonian

$$\mathcal{H} = - \sum_{l,i,j,\alpha} t_l (c_{l,i,\alpha}^\dagger c_{l,j,\alpha} + \text{H.c.}) - \sum_{l,I} J_l \mathbf{S}_I \cdot \mathbf{s}_{l,I}, \quad (1)$$

where  $l=1,2$  is the band index (not to be confused with angular momentum),  $i, j$  label sites (nearest neighbors for the hopping term),  $c_{l,i,\alpha}$  creates a hole at site  $i$  in the band  $l$ ,  $\mathbf{s}_{l,i} = \sum_{\alpha,\beta} \sigma_{\alpha\beta} c_{l,i,\alpha}^\dagger c_{l,i,\beta}$  is the spin-operator of the mobile hole ( $\hat{\sigma}$ =Pauli vector),  $\alpha$  and  $\beta$  are spin indices,  $J_l$  is the coupling between the core spin and the electrons of band  $l$ , and  $\mathbf{S}_I$  is

the spin of the localized Mn ion at randomly selected sites  $I$ , assumed classical in the MC simulations.  $t_l$  is the hopping term in band  $l$ . The interband hopping  $t_{12}$  ( $=t_{21}$ ) is zero at the nearest-neighbor level in cubic lattices.<sup>9</sup> Even if  $t_{12}$  is explicitly added, the conclusions are similar as reported here.<sup>10</sup> While real DMS materials have zinc-blende (ZB) structures, in this nonperturbative study of a multiband DMS model the simplicity of a cubic lattice allows us to focus on the dominant qualitative tendencies, a first step toward future quantitative studies with realistic ZB lattices. The model will be studied using DMFT and MC techniques.

### III. DMFT RESULTS

#### A. Formalism and tests

Within DMFT the self-energy is assumed to be local,  $\Sigma(\mathbf{p}, i\omega_n) \rightarrow \Sigma(i\omega_n)$ , valid exactly only in infinite dimensions.

$$-\sum_{l=1}^2 \sum_{n=0}^{\infty} \frac{4xJ_l^2 W_l^2 B_l^2(i\omega_n)}{48[B_l^2(i\omega_n) - J_l^2]^3 + (48J_l^2 - 3W_l^2)[B_l^2(i\omega_n) - J_l^2]^2 - 5xJ_l^2 W_l^2 [B_l^2(i\omega_n) - J_l^2] - 2xJ_l^4 W_l^2} = 1, \quad (2)$$

where  $B_l(i\omega_n)$  satisfies a fourth-order-degree equation:  $B_l^4 - z_n B_l^3 - (J_l^2 - W_l^2/16)B_l^2 + z_n J_l^2 B_l - (1-x)J^2 W_l^2/4 = 0$ .<sup>10</sup> Our formula was tested in different cases: (1) for  $J_2=0$ , we reproduce the one-band results of Ref. 2, and (2) at  $x=1$ ,  $J_2=0$ , and  $J_1 \rightarrow \infty$  we reproduced the results of Ref. 11.  $T_c$ , contained in the Matsubara frequencies, is obtained from Eq. (2) numerically. The equations for  $B_l$ , rewritten in real frequency space via  $i\omega_n \rightarrow \omega$ , give the interacting DOS for each band at zero temperature when  $\mu=0$ .<sup>12</sup> The solutions of these equations depend crucially on the ratio  $J_l/W_l$ . The critical value for the formation of well-defined IB, corresponding to carrier spins locally parallel to Mn spins, is  $J_l/W_l \sim 0.33$ . Below, the domain  $J_l/W_l < 0.33$  is referred to as “weak coupling,” while  $0.33 \leq J_l/W_l \leq 0.5$  is the “intermediate coupling.” The most interesting physics was observed at the boundary between these two regimes, i.e., when the IB are not completely separated from the valence bands.

#### B. DMFT critical temperatures varying exchange couplings

In Fig. 1, we show  $T_c$  vs  $p$ , for different ratios  $J_2/J_1$  and at fixed  $W_2/W_1=1$  and  $J_1/W_1=0.5$ , a situation corresponding to the existence of a well-defined  $l=1$  IB (although  $p \leq x$  in real DMS, in this paper the case  $p > 1$  will also be studied for completeness, as done in Ref. 2). The inset shows the total interacting DOS evolution. The IB overlap if  $|J_2/W_2 - J_1/W_1| < 0.5$ . If the IB do not overlap, then each one determines  $T_c$  separately, causing the double-peak structure observed for some  $J_2/J_1$  ratios. The band with the largest  $J_l/W_l$  is filled first, for smaller  $\mu$ 's. At all  $p$ 's, we found that  $T_c$  is maximum when  $J_2/J_1=1$ , namely when the IB fully overlap. The dependence of  $T_c$  on  $J_2/J_1$  at fixed  $p$  is in Fig. 2(a). The

The information about the hopping of carriers on and off lattice sites, which are magnetic (with probability  $x$ ) or nonmagnetic (with probability  $1-x$ ), is in the bare Green's function (GF)  $\mathcal{G}_0(i\omega_n)$ .<sup>6</sup> The full GF  $\mathcal{G}(i\omega_n)$  can be solved by integration with the result:  $\langle \mathcal{G}(i\omega_n) \rangle = x \langle [\mathcal{G}_0^{-1}(i\omega_n) + J\mathbf{S}\mathbf{m}\hat{\sigma}]^{-1} \rangle + (1-x) \langle \mathcal{G}_0(i\omega_n) \rangle$ , where  $\omega_n = (2n+1)\pi T$  are Matsubara frequencies. The average  $\langle X(\mathbf{m}) \rangle = \int d\Omega_m X(\mathbf{m}) P(\mathbf{m})$  is over the local moment  $\mathbf{m}$  orientations, with probability  $P(\mathbf{m})$ . The equation above was derived for each band, and the equations set for the GF were solved on a Bethe lattice with a bare semicircular noninteracting density of states  $\text{DOS} = 8(W_l^2/4 - \varepsilon^2)^{1/2}/\pi W_l^2$ . In this case,  $\langle \mathcal{G}_{0,l}^{-1}(i\omega_n) \rangle = z_n - (W_l^2/16) \langle \mathcal{G}_l(i\omega_n) \rangle$ , where  $z_n = i\omega_n + \mu$ , and  $W_l = 4t_l$ .  $T_c$  is obtained by linearizing the bare inverse GF with respect to the local order parameter  $M = \langle m_z \rangle_{\mathbf{m}}$ . To first order in  $M$ , the equation for  $T_c$  is

peak value is achieved when the bands fully overlap (i.e., at  $J_2/J_1=1$ ). Once the bands decouple, the value for  $T_c$  matches one-band model results.

#### C. DMFT critical temperatures varying bandwidths

Let us consider now how changes in bandwidths influence  $T_c$ . In Fig. 2(c), we show  $T_c$  vs  $p$  parametric with  $W_2/W_1$ , at fixed  $J_1/W_1=0.5$  (intermediate coupling), and with  $J_2/J_1=1$ .<sup>13</sup> At small  $W_2/W_1$  the second IB shall be located in

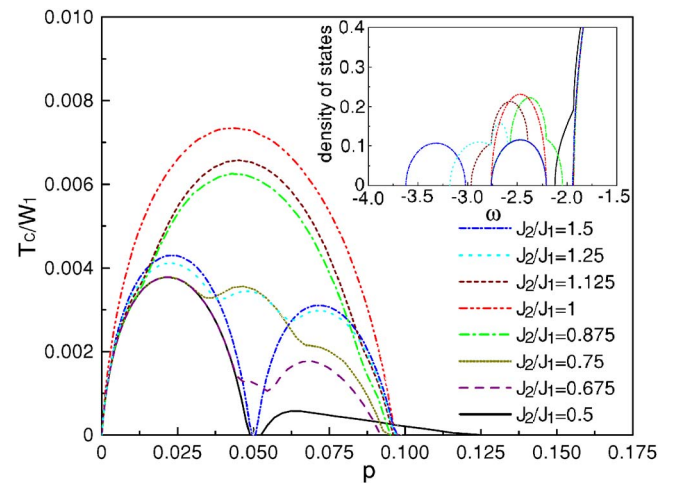
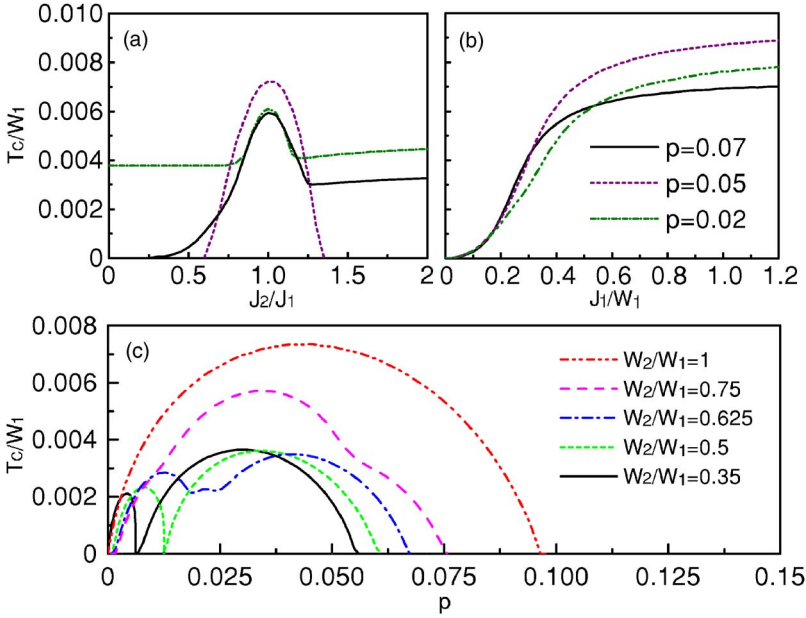


FIG. 1. (Color online)  $T_c$  vs the carrier concentration  $p$ , at various  $J_2/J_1$ , obtained with the DMFT technique. Here,  $x=0.05$ ,  $W_1/W_2=1$ , and  $J_1/W_1=0.5$ . The inset shows the corresponding DOS at  $T=0$ .



a region of  $\omega$  smaller (i.e., farther from the valence bands) than the energy interval occupied by the  $l=1$  IB. Hence the  $l=2$  IB will be the first to be filled. Decreasing  $J_2/W_2$ , the second band moves to the right on the  $\omega$  axis, towards the location of the first band. While the bands are still separated, each gives its own contribution to  $T_c$ . The curves with  $W_2/W_1=0.35$  and  $0.5$  correspond to decoupled IB, while those with  $W_2/W_1=0.625$  and  $0.75$  correspond to partially overlapping bands. Again,  $T_c$  is maximized at all fillings when the bands fully overlap ( $W_2/W_1=1$ ), in good agreement with Ref. 6. Although  $W_2/W_1=1$  is not realistic in DMS, Mn doping materials with a relatively small heavy-light mass ratio will favor a higher  $T_c$ .

#### D. Critical temperatures varying the exchange-to-bandwidth ratio

Once it is established that  $T_c$  is maximal for all  $p$  when  $J_2/J_1=1$  and  $W_2/W_1=1$ , let us analyze  $T_c$  vs  $p$  when  $J_1/W_1$  varies. The results for  $T_c$ , and total interacting DOS, are in Fig. 3. At small coupling  $J_1/W_1 \ll 0.33$ ,  $T_c$  is small, flat, and much extended on the  $p$  axis, qualitatively similar to the one-band results.<sup>2</sup> However, at intermediate coupling,  $T_c$  is nonzero in the range from  $p=0$  to  $p=2x$ , adopting a parabolic form with the maximum at  $p \cong x$ , in contrast with the one-band model which gives a null  $T_c$  when  $p \cong x$ . The explanation is straightforward: at  $p=x$  in the one-band model the IB is fully occupied leading to a vanishing  $T_c$ , but for the same  $p$  in the two-band model both bands are half filled, which ultimately leads to the highest value for  $T_c$ . The  $T_c$  dependence on the ratio  $J_1/W_1$  at some fillings  $p$  is displayed in Fig. 2(b). At small coupling,  $T_c$  correctly increases quadratically with  $J_1/W_1$ , but at strong coupling  $T_c$  incorrectly continues growing, a result which will be improved upon by the MC simulations shown below.

#### IV. MONTE CARLO RESULTS

The Hamiltonian Eq. (1) was also studied numerically using MC techniques similar to those applied to Mn-oxide

investigations.<sup>3,14</sup> The fermionic sector is treated exactly, while a MC simulation is applied to the classical localized spins. Cubic lattices with  $5^3$  and  $6^3$  sites were investigated. These lattice sizes have been shown to be sufficient for the comparison with DMFT results and to unveil general trends. In addition, the figures show only small variations for the  $T_c$  estimations using the two lattices. However, if more sophisticated quantitative analysis is required, clearly larger systems will be needed. One may suspect that actually the number of Mn spins may regulate the size effects, rather than the number of sites. For the small values of  $x$  used in our study, the number of Mn spins is also very small and serious size effects could be expected. However, in practice this does not seem to occur, and, moreover, the comparison with DMFT shows similar results using both techniques. Perhaps in the small  $J$ 's regime, the delocalized nature of the carriers smears the effects caused by the actual location of the Mn spins. These issues deserve further study, but for our purposes of unveiling trends in the multiparameter space of

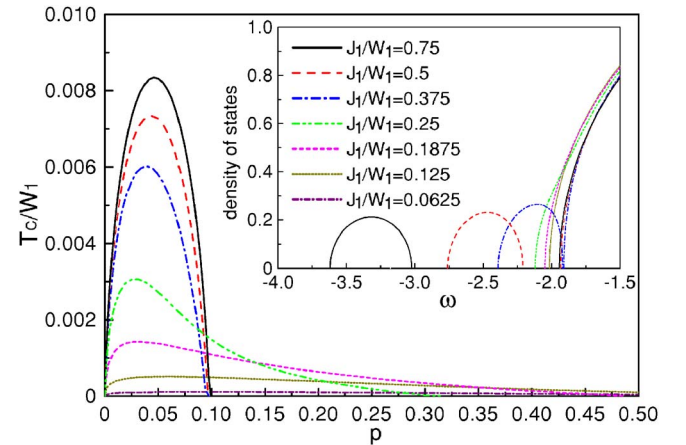


FIG. 3. (Color online)  $T_c$  vs  $p$  at different ratios  $J_1/W_1$ , obtained using DMFT. The parameters  $x$ ,  $W_1$ ,  $W_2$ , and  $J_1$  are as in Fig. 1. The inset contains the DOS at  $T=0$ .

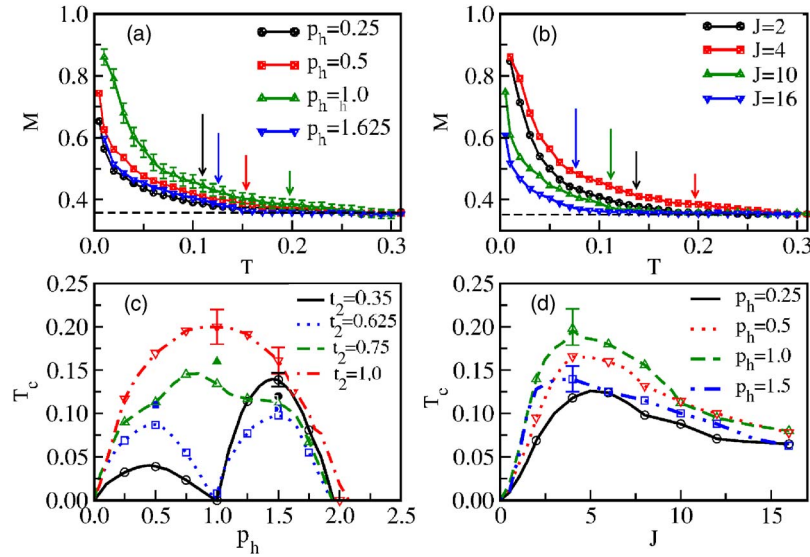


FIG. 4. (Color online) (a) MC magnetization (in absolute value) vs temperature ( $T$ ), with  $J_1=J_2=4$  and  $t_1=t_2=1$ , for the hole densities indicated. The dashed line is the exact asymptotic high-temperature value  $M_\infty$ , which tends to 0 only in the bulk limit. In this paper, the  $T_c$  on the  $5^3$  cluster was (arbitrarily) defined as the  $T$  where  $M$  reaches  $\sim 5\%$  of the  $1-M_\infty$  value [indicated by arrows in (a) and (b)]. Other criteria lead to very similar conclusions. (b) Magnetization vs  $T$  for  $p_h=1$ ,  $t_1=t_2$ , and several (equal) magnetic couplings  $J$ . (c) Curie temperature vs hole density for  $J=4$  and different ratios of the band hoppings. (d) Curie temperature versus the (equal) magnetic interactions  $J$  for several hole densities and equal band hoppings  $t_1$  and  $t_2$ . Results for  $6^3$  ( $5^3$ ) lattices are indicated by closed (open) symbols. Error bars due to the disorder (up to seven samples) are only shown for a few points for clarity.

DMS materials, the lattices used here are sufficient.

Returning to the numerical data, the spin magnetization is the order parameter that was used to detect the ferromagnetic transition.<sup>14</sup> All quantities are in units of  $t_1=1$ , and the density of magnetic impurities is  $x \approx 0.065$ . In Fig. 4(a), typical magnetization curves are presented at several carrier densities  $p_h$ , and for  $J_1=J_2=J=4$  and  $t_2=1$ . In excellent agreement with DMFT, it was observed that the estimated  $T_c$  is the highest for  $p_h=1$ . The value of  $J$  used maximizes the critical temperature, and it was confirmed that it corresponds to the case where the IB are about to become separated from the valence band. In Fig. 4(b), it is shown how  $T_c$  increases with  $J$  up to  $J=4$ , in agreement with DMFT. The strong coupling behavior is nevertheless different since  $T_c$  decreases at large  $J$ . This is caused by hole localization in strong coupling,<sup>3</sup> beyond the capabilities of DMFT. The dependence of  $T_c$  on the ratio of band hoppings is in Fig. 4(c), varying  $p_h$ . These results are again in good qualitative agreement with DMFT [Fig. 2(c)]. The maximum  $T_c$  for all values of  $p_h$  occurs when  $t_2/t_1=1$ . However, when  $t_2$  is very different from  $t_1$  the development of magnetism is regulated by only one of the IB and the results are similar to those obtained with a single band model, as shown in the curves for  $t_2=0.35$  and  $0.625$  in Fig. 4(c). For  $t_2/t_1$  closer to 1, a partial overlap of the IB occurs and a hump in  $T_c$  develops at  $p_h=1$  (see curve for  $t_2=0.75$ ).

In Fig. 4(d) we show that, once  $t_2/t_1$  is optimized, a similar finite  $J$  maximizes  $T_c$  for several  $p_h$ 's. In all cases, the optimal  $J$  best balances the weak coupling behavior, with mobile holes not much affected by the interaction with the Mn ions, and the strong coupling region where the hole spins strongly align with the Mn spins, becoming localized. This “sweet spot” is achieved when the IB are about to be separated from the valence bands.

$T_c$  vs  $p_h$ , at several ratios  $J_2/J_1$  and for  $t_1=t_2$  is presented in Fig. 5(a). In agreement with DMFT (Fig. 1),  $T_c$  is maximized for all values of  $p_h$  if  $J_2=J_1$ , with the highest value at  $p_h=1$ . Overall, there is an excellent agreement with DMFT, as described in the caption.<sup>15</sup>  $T_c$  vs  $p_h$  for several  $J_1=J_2=J$  is in Fig. 5(b). At small  $J$ , again the MC results resemble those obtained with DMFT (Fig. 3). For, e.g.,  $J=2$  the IB are not formed yet (inset). In this regime,  $T_c$  remains finite, although small, even for  $p_h$  larger than 2. Increasing  $J$ , a nonzero  $T_c$  is obtained only for  $p_h$  between 0 and 2, due to IB formation.  $T_c$  reaches a maximum at  $J=4$ .

## V. CONCLUSIONS

We have carried out the first study of a multiband model for DMS using a powerful combination of nonperturbative techniques, DMFT and MC. We found the parameter regime that maximizes  $T_c$ . This happens at intermediate couplings and for all hole densities when  $J_1/J_2=1$  and  $W_1/W_2=1$ . The maximum  $T_c$  is obtained at  $p \cong x$ , in contrast with the one-band model which has a vanishing  $T_c$  at the same doping. In addition,  $T_c$  at filling  $p \cong x/2$  in the one-band case is smaller than with two bands by a factor of  $\sim 2$ . In view of the simplicity of the main results, it is clear that adding an extra band to the calculations (which is relevant for a system with negligible SO, but considerably raises the CPU cost) will only lead to a further increase in  $T_c$  when all the IB overlap.

The excellent agreement DMFT-MC is somewhat surprising due to the fact that Monte Carlo considers the influence of the random location of the Mn sites much better than DMFT. However, at small and intermediate  $J$ 's, the carriers can be sufficiently delocalized that a smearing effect may occur and considering the quenched disorder only in average

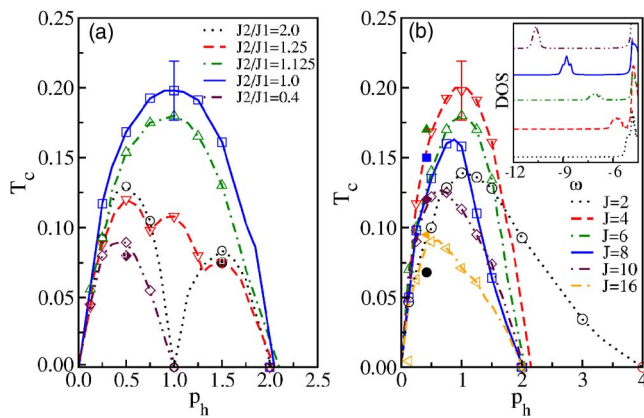


FIG. 5. (Color online) (a)  $T_c$  vs  $p_h$  obtained with MC on a  $6^3$  ( $5^3$ ) lattice with  $t_1=t_2=1$  for the values of  $J_2/J_1$  indicated by the closed (open) symbols.  $J_1$  is fixed to 4, i.e., when the IB are about to separate from the valence band for band 1 [inset Fig. 5(b)]. For  $J_2 < J_1$  (e.g.,  $J_2/J_1=0.4$  curve),  $T_c$  is regulated by the IB in band 1, since the IB for band 2 is deep into the valence band. In this case, a single-band behavior is observed, with  $T_c$  maximized for  $p_h=0.5$ . For  $J_2 > J_1$ , both IB play a role. For  $J_2 \gg J_1$  (see  $J_2/J_1=2$ ), the two IB do not overlap, and for  $0 \leq p_h \leq 1T_c$  is determined by the band-2 IB reaching a maximum at  $p_h=0.5$  and vanishing at  $p_h=1$ . For larger  $p_h$ ,  $T_c$  is controlled now by the IB 1, and it raises again passing through a maximum at  $p_h=1.5$  and vanishing at  $p_h=2$ . For  $J_2/J_1=1.25$ , the two IB overlap and we observe residual local maxima at  $p_h=0.5$  and  $1.5$ , related to the single band physics, and a new local maximum at  $p_h=1$  due to IB overlap for the corresponding value of the chemical potential.  $T_c$  at  $p_h=0.5$  is boosted by the partial IB overlap as well. (b)  $T_c$  vs  $p_h$  for  $t_2/t_1=1$  and several  $J$ 's. Inset: low- $T$  DOS.

appears to be sufficient. Certainly at large  $J$ 's the MC and DMFT methods give totally different answers, with MC capturing the correct localization result.

The approach described here is also quantitative. In fact, using GaAs realistic parameters such as  $p=0.005$  ( $p_h=0.1/\text{Mn}$ ), a bandwidth  $\sim 10$  eV ( $t_1=2.5$  eV),  $t_2=(1/9)t_1$ , and assuming  $J_1/t_1=1$  and  $J_1=J_2$ , we obtain  $T_c \approx 175$  K, i.e., within the experimental range. While this excellent agreement with experiment may be accidental, the trends are reliable and the result improves upon single-band estimations. Moreover, for optimal  $t_2/t_1=1$  and  $J_1/t_1=2$ , the  $T_c$  raises to  $\sim 340$  K, even at small  $p_h=0.1$ , setting the upper bound for DMS under a two-band model description using a cubic lattice.

The general qualitative picture presented here can be used to search for DMS with even higher  $T_c$ 's than currently known. Our results suggest that semiconductors with the smallest heavy-to-light hole mass ratio, such as AlAs, could have the highest  $T_c$  if the couplings  $J$  could be tuned to its optimal value. The present effort paves the way toward future nonperturbative studies of DMS models using realistic ZB lattices, and points toward procedures to further increase the Curie temperatures.

#### ACKNOWLEDGMENTS

We acknowledge conversations with K. Aryanpour, M. Berciu, R. Fishman, J. Moreno, and J. Schliemann. This research was supported by Grant No. NSF-DMR-0443144. ORNL is managed by UT-Battelle, LLC under Contract No. De-AC05-00OR22725. MC simulations used the SPF program (<http://mri-fre.ornl.gov/spf>).

- <sup>1</sup>H. Ohno, *Science* **281**, 951 (1998); T. Dietl, H. Ohno, F. Matsukura, J. Cibert, and D. Ferrand, *ibid.* **287**, 1019 (2000); S. J. Potashnik, K. C. Ku, S. H. Chun, J. J. Berry, N. Samarth, and P. Schiffer, *Appl. Phys. Lett.* **79**, 1495 (2001).
- <sup>2</sup>A. Chattopadhyay, S. Das Sarma, and A. J. Millis, *Phys. Rev. Lett.* **87**, 227202 (2001), and references therein. For a DMFT review, see A. Georges, G. Kotliar, W. Krauth, and M. J. Rozenberg, *Rev. Mod. Phys.* **68**, 13 (1996).
- <sup>3</sup>G. Alvarez, M. Mayr, and E. Dagotto, *Phys. Rev. Lett.* **89**, 277202 (2002); *Phys. Rev. B* **68**, 045202 (2003).
- <sup>4</sup>J. Sinova, T. Jungwirth, S. R. Eric Yang, J. Kucera, and A. H. MacDonald, *Phys. Rev. B* **66**, 041202(R) (2002); T. Jungwirth, J. Konig, J. Sinova, J. Kucera, and A. H. MacDonald, *ibid.* **66**, 012402 (2002).
- <sup>5</sup>J. Schliemann, J. Konig, and A. H. MacDonald, *Phys. Rev. B* **64**, 165201 (2001), MC studies of multiband models at small  $J$  were presented but without using an underlying lattice and replacing the fermion trace by a ground state expectation value.
- <sup>6</sup>K. Aryanpour, J. Moreno, M. Jarrell, and R. S. Fishman, *Phys. Rev. B* **72**, 045343 (2005); J. Moreno, R. S. Fishman, and M. Jarrell, *cond-mat/0507487* (unpublished).
- <sup>7</sup>The term ‘‘impurity band’’ is widely used in the DMS literature [see, e.g., M. Berciu and R. N. Bhatt, *Phys. Rev. Lett.* **87**, 107203 (2001); J. Okabayashi, A. Kimura, O. Rader, T. Mi-

zokawa, A. Fujimori, T. Hayashi, and M. Tanaka, *Phys. Rev. B* **64**, 125304 (2001)], although it should not be confused with the same term used in nonmagnetic doped semiconductor literature. Perhaps ‘‘exchange split valence band’’ could be better terminology.

- <sup>8</sup>G. Zarand and B. Janko, *Phys. Rev. Lett.* **89**, 047201 (2002). In Ref. 6 it was shown that the frustration can be turned off by giving equal masses to the light and heavy sectors. Our emphasis has been on this particular case, since under this circumstance the  $T_c$  is maximized.
- <sup>9</sup>A. Moreo (unpublished).
- <sup>10</sup>Details will be published elsewhere.
- <sup>11</sup>R. S. Fishman and M. Jarrell, *Phys. Rev. B* **67**, 100403(R) (2003).
- <sup>12</sup>The interacting DOS is  $-(2/\pi)\sum_{l=1}^2 \text{Im}[B_l(\omega) - \omega]$ .
- <sup>13</sup>The relative position of the bands is fixed by shifting numerically the  $l=2$  valence band such that both valence bands start at the same energy, to mimic the degeneracy of the light and heavy bands of GaAs at  $\Gamma$ .
- <sup>14</sup>E. Dagotto, T. Hotta, and A. Moreo, *Phys. Rep.* **344**, 1 (2001).
- <sup>15</sup>This agreement is even quantitative for the optimal  $T_c$  and  $J$  coupling, once the factor  $\sqrt{2d}$  ( $d$ =dimension), used to rescale the hopping in DMFT, is considered.